

Dynamic Analysis of the Perforation of Aluminum Alloy at Low Velocity Impact

S. Koubaa, J. Mars, M. Wali and F. Dammak

Abstract A finite element implementation of an anisotropic plasticity model for aluminum AA5754-O in impact simulations was performed, particularly for the case of perforation on low velocity (up to about 25 m/s). The elasto-viscoplastic model includes isotropic elasticity, anisotropic yielding, associated plastic flow and mixed non-linear isotropic/kinematic hardening. Coupling between elasto-viscoplastic model and isotropic ductile damage is investigated. Strain rate is integrated in numerical modeling. The material model is implemented into a user-defined material (VUMAT) subroutine for the commercial finite element code ABAQUS/Explicit to predict the numerical response of circular aluminum plate subjected to low velocity impact. Results include the effect of anisotropy on the material behavior. It is shown that anisotropy plays a significant role in penetration of the present plate material.

Keywords Dynamic analysis · Impact velocity · Perforation · Aluminum · Damage · Strain rate · Anisotropy

S. Koubaa (✉) · J. Mars · M. Wali · F. Dammak
Mechanical Modeling and Manufacturing Laboratory (LA2MP), National Engineering
School of Sfax, University of Sfax, B.P W3038, Sfax, Tunisia
e-mail: koubaasana@yahoo.fr

J. Mars
e-mail: jamelmars@yahoo.fr

M. Wali
e-mail: mondherwali@yahoo.fr

F. Dammak
e-mail: fakhreddine.dammak@enis.rnu.tn

1 Introduction

Nowadays, structural impact engineering is a common field in sectors as nuclear, chemical, transport, offshore, naval, aerospace, defense and process industries. The study of the response of structures subjected to intense dynamic loads, which produce large inelastic deformation, and failure has become increasingly important in structural design and safety calculation. The literature on impact loading includes a variety of materials, thicknesses and projectile geometries, as well as velocity ranges from low (Fagerholt et al. 2010; Mohotti et al. 2014; Grytten et al. 2009) to intense impact (Mohotti et al. 2013).

It is well known that the energy absorption capacity per unit density of aluminum is high when compared to conventional steel. Therefore, accurate constitutive models for aluminum alloys have been of significant interest.

A particular case of structural impact by missiles or projectiles is perforation of metal plating. Many articles were written on the perforation of aluminum plates for various ranges of velocities, (Marvin et al. 1978, Wilkins 1978; Corran et al. 1983, Iqbal et al. 2006). In the past, more attention was given to experimentally investigate the impact behavior of target and projectile (Børvik et al. 2004) and to construct approximate analytical models (Børvik et al. 2009). For instance, Jones and Paik (2012) focused on the low-velocity (up to about 20 m/s) and moderate-velocity (20–300 m/s, approximately) perforation of steel plates struck by projectiles having cylindrical bodies and various shaped impact faces. Nevertheless, few reported studies exist in which experimental results are directly compared with those found from finite element simulation. In numerical studies, the Johnson Cook phenomenological behavior law of the plate's material was considered (Antoinat et al. 2015; Iqbal et al. 2010; Rodriguez-Martinez et al. 2012; Dean et al. 2009; Abdulhamid et al. 2013; Børvik et al. 2009). Nevertheless, the anisotropy is an important aspect that should be taken into account when modeling inelastic materials impact behavior. Few studies were interested in anisotropy (Grytten et al. 2009; Barlat et al. 2005). A recent article (Mars et al. 2015) has discussed the influence of anisotropy on low velocity impact on aluminum plates.

This article is concerned primarily with finite element simulation of the perforation of aluminum alloy plates struck by projectiles travelling at low-initial impact velocities (say up to about 25 m/s). For this, a two-equation integration algorithm of a generalized quadratic yield criterion of Hill based on the mixed non-linear isotropic/kinematic hardening models of Chaboche is developed for computing elasto-viscoplastic stress during impact. The strain rate effect is integrated. The isotropic damage model is considered. The numerical simulation of the perforation problem is carried out using the commercial software ABAQUS/Explicit. The material constitutive law is implemented in a user-subroutine VUMAT. The effect of anisotropy on low velocity impact of aluminum plates is investigated so that a comparison is made between simulation results of the developed model and that derived from Johnson-Cook behavior.

2 Numerical Simulation

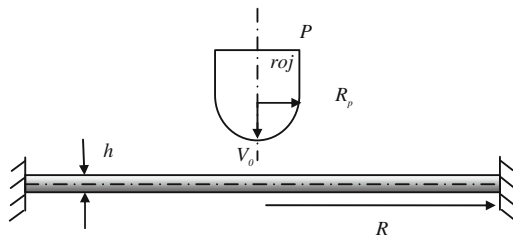
In this section, numerical simulations are conducted on the perforation of aluminum alloy plates struck by rigid hemispherical-nosed projectiles, using dynamic finite element code ABAQUS/Explicit. The target was modeled using the elasto-viscoplastic constitutive relation, which was implemented as a user-defined material model by means of a subroutine (VUMAT).

2.1 Finite Element Model

A clamped circular plate impacted at its center by a cylindrical impactor with hemispherical nose is considered. The proposed finite element models of projectiles are shown in Fig. 1. The projectile has the diameter of 6.35 mm and the circular shape of target aluminum plate has the radius of 60 and 0.5 mm thickness. The initial velocity of impactor is V_0 . The deformation of the striker during impact is neglected and so it can be modeled as an analytical rigid surface with an associated mass reference point.

A 3D finite element model for the simulation of the penetration process was developed ABAQUS/VUMAT. The modeling is carried out by taking into account the geometric symmetry of the circular plate. Indeed, in three dimensional analyses, only the $\frac{1}{4}$ of plate is taken into account in the impact analysis. The plate is meshed using 40000 C3D8R elements (8_node linear brick, reduced integration with hourglass control). Mesh pattern of the area surrounding the contact region is depicted in Fig. 2 (0.4 mm in radius direction and 5 elements in thickness). Obviously, accurate results required fine mesh beneath the contact area and all the meshes contained three regions: a finely zoned region which had noticeable effect on computational accuracy, a coarsely zoned region which did not have noticeable effect on computational accuracy, and a transitional region between the two regions above. The element size in transitional region and coarsely zoned region was increased from the central part to the outer part of the target.

Fig. 1 Cylindrical projectile impacted circular plate



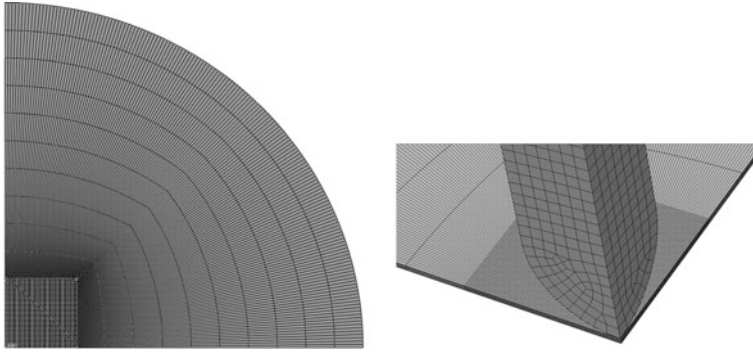


Fig. 2 Three-dimensional problem: rigid impactor

A hard contact law is used for modeling the contact. To define contact interactions, the default finite-sliding formulation (surface to surface contact) is used. In order to define the boundary conditions for the impactor, the movement of the impactor is restrained in all directions except translation along normal vector of the plate. The validation of contact model was assessed in Mars et al. (2015).

2.2 Constitutive Relations

According to the damage model of Lemaitre and Chaboche (1990), the Helmholtz free energy is taken as the thermodynamic potential or state potential and is defined as

$$\begin{aligned} \psi(\varepsilon^e, \alpha_k, r, d) &= \psi^e(\varepsilon^e, d) + \psi^p(\alpha_k, r) \\ &= \frac{1}{2}(1-d) \varepsilon^e : \mathbf{D} : \varepsilon^e + \psi_{iso}(r) + \frac{1}{2} \sum_{k=1}^M a_k \alpha_k : \alpha_k \end{aligned} \quad (1)$$

where α_k and r are internal variables corresponding to kinematics and isotropic hardening respectively and d is the damage variable.

The Chaboche model is based on the assumption of the strain additivity

$$\boldsymbol{\varepsilon} = \boldsymbol{\varepsilon}^e + \boldsymbol{\varepsilon}^p \quad (2)$$

The thermodynamic forces associated with the internal variables can be determined as

$$\boldsymbol{\sigma} = \frac{\partial \psi}{\partial \boldsymbol{\varepsilon}^e} = (1 - d)\mathbf{D} : \boldsymbol{\varepsilon}^e \tag{3}$$

$$\mathbf{X}_k = \frac{\partial \psi}{\partial \boldsymbol{\alpha}_k} = a_k \boldsymbol{\alpha}_k \tag{4}$$

$$R = \frac{\partial \psi}{\partial r} \tag{5}$$

$$Y = -\frac{\partial \psi}{\partial d} = \frac{1}{2} \boldsymbol{\varepsilon}^e : \mathbf{D} : \boldsymbol{\varepsilon}^e \tag{6}$$

where $\boldsymbol{\sigma}$ is the stress tensor, \mathbf{D} is the general elastic operator, $\psi_{iso}(r)$ represents the potential associated with isotropic hardening, R is the thermodynamic force associated with isotropic hardening, which is an arbitrary scalar function of the isotropic internal variable, r , \mathbf{X} represents the so-called back-stress tensor and Y is the thermodynamic force associated with damage.

The evolution equations for all the internal variables are derived from complementary dissipation potential, as

$$\dot{\boldsymbol{\varepsilon}}^p = \dot{\gamma} \frac{\partial F}{\partial \boldsymbol{\sigma}} = \frac{\dot{\gamma} \sqrt{3/2}}{(1 - d)^\delta} \mathbf{n}, \mathbf{n} = \frac{1}{\varphi} \mathbf{P} \boldsymbol{\xi}, \boldsymbol{\xi} = \boldsymbol{\sigma} - \mathbf{X} \tag{7}$$

$$\dot{\boldsymbol{\alpha}}_k = -\dot{\gamma} \frac{\partial F}{\partial \mathbf{X}} = \dot{\boldsymbol{\varepsilon}}^p - \dot{\gamma} \frac{b_k}{a_k} \mathbf{X}_k \tag{8}$$

$$\dot{r} = -\dot{\gamma} \frac{\partial F}{\partial R} = \dot{\gamma} \tag{9}$$

$$\dot{d} = \dot{\gamma} \frac{\partial F}{\partial Y} = \dot{\gamma} \bar{Y}, \bar{Y} = \frac{1}{(1 - d)^\beta} \left(\frac{1 - d}{1 - \bar{h}d} \right)^{2s} \left\langle \frac{Y - Y_0}{S} \right\rangle^s, \begin{cases} \bar{h} = 1 & \text{if } \eta \geq 0 \\ \bar{h} = h & \text{if } \eta < 0 \end{cases} \tag{10}$$

where $\dot{\gamma}$ is the plastic multiplier, $\varphi = \|\boldsymbol{\xi}\|_p = \sqrt{\boldsymbol{\xi}^t \mathbf{P} \boldsymbol{\xi}}$ is a generalized quadratic yield function, \mathbf{P} is a fourth order tensor, β, s, S, Y_0 and $h \in [0, 1]$ are material parameters and η is the stress triaxiality. The notation $\langle x \rangle$ indicates the positive value of x i.e. $\langle x \rangle = x$ if $x > 0$ and $\langle x \rangle = 0$ if $x \leq 0$.

In three-dimensional cases, it is given by

$$\mathbf{P} = \frac{2}{3} \begin{bmatrix} H + G & -H & -G & 0 & 0 & 0 \\ & H + F & -F & 0 & 0 & 0 \\ & & F + G & 0 & 0 & 0 \\ & & & 2N & 0 & 0 \\ & \text{Sym} & & & 2M & 0 \\ & & & & & 2L \end{bmatrix} \tag{11}$$

where F , G , H , N , M and L are material constants obtained by tests of the material in different orientations. The J_2 plasticity yield criterion is recovered using

$$F = G = H = 0.5, N = M = L = 1.5 \quad (12)$$

Finally, by using the fully implicit backward Euler integration procedure, the coupled elastoplastic-damage model is reduced to two scalar equations as

$$\begin{cases} f_1(\Delta\gamma, d) = \frac{\sqrt{3/2}\varphi}{(1-d)^{\delta}} - \sigma_p = 0 \\ f_2(\Delta\gamma, d) = d - d_n - \Delta\gamma\bar{Y} = 0 \end{cases} \quad (13)$$

The unknowns of this system of equations are the plastic multiplier $\Delta\gamma$ and the damage variable d . The system of equations, Eq. (13), is solved with the Newton-Raphson method. More details can be found in Wali et al. (2015a, b).

2.3 Extension to Viscoplasticity

Structural impact involves events such as plastic flow at high strain rates, possible local increase of temperature, and material fracture. In this paper, the loading/unloading condition, Eq. (13), for rate dependent plasticity is rewritten in terms of the function $g(\cdot)$ as

$$f_1 = g\left(\frac{\Delta\gamma}{\Delta t}\right) \quad \text{for } f_1 > 0 \Leftrightarrow \Delta\gamma > 0 \quad (14)$$

Combining Eq. (13) with the consistency condition Eq. (14) gives the modified system as

$$\begin{cases} h_1(\Delta\gamma, d) = \frac{\sqrt{3/2}\varphi}{(1-d)^{\delta}} - \left[\sigma_p + g\left(\frac{\Delta\gamma}{\Delta t}\right)\right] = 0 \\ h_2(\Delta\gamma, d) = d - d_n - \Delta\gamma\bar{Y} = 0 \end{cases} \quad (15)$$

Instead, simple models, to introduce the rate dependent plasticity, consisting of rather few parameters seem to be more popular. One of the most frequently used in impact problems is the Johnson-Cook model. In this case, the function g is written as

$$g\left(\frac{\Delta\gamma}{\Delta t}\right) = C\sigma_p \text{Log}\left(\frac{\Delta\gamma}{\Delta t}\right) \quad (16)$$

According to Smerd et al. (2005), the estimated C-value of AA5754-O is equal to 0.004556.

3 Simulation Results

Numerical simulations were carried out to study the response of Aluminum AA5754-O target subjected to low velocity impact of hemispherical nosed projectiles. The effect of anisotropy is studied by comparing the two elasto-plastic models: J_2 and Hill yield criteria with isotropic and mixed non-linear isotropic/kinematic hardening models, IH and NKH, respectively. The mechanical properties of both Aluminum plate are gathered in Table 1. Hardening parameters of the aluminum AA5754-O material are presented in Table 2. The initial impact velocity was 25 m/s.

Figure 3 depicts the failure of aluminum plate at different stages. The beginning of the petalling process during perforation is always associated with fracture initiation and the outward move of petals as perforation continues. At the time step 0.56 ms, when using J_2 -IH, dishing formation occurs and the following motion of projectiles leads to the crack propagation of the impacted surface. At the same time, for the case of Hill-NKH, the projectile body is already passed through the perforated surface and the petal formation generated around it as shown in Fig. 3. It is clear that the final form of the petal bending is different for the two models. Hence, anisotropy seems to have an effect on material behavior on low impact velocity. The resulting force versus time curves are compared when considering the Von Mises yield criterion with IH and the anisotropic Hill criterion with NKH. Figure 5 shows an important difference between the isotropic and anisotropic models as the force level is affected. This is in a good agreement with results in Figs. 3 and 5, as perforation appears more rapidly in the second case (Fig. 4).

Table 1 Mechanical properties of the aluminum AA5754-O material

Elastic Prop.		Hill'48 coefficients				Damage data		
E (GPa)	ν	F	G	H	N	s	S	δ
70	0.33	0.748	0.572	0.403	1.467	1.0	1.25	1

Table 2 Hardening parameters of the aluminum AA5754-O material

Parameter	IH	NKH
σ_y (MPa)	95	95
Q (MPa)	159	92.6
β	9	11
a (MPa)	–	1291
b_1	–	35.8

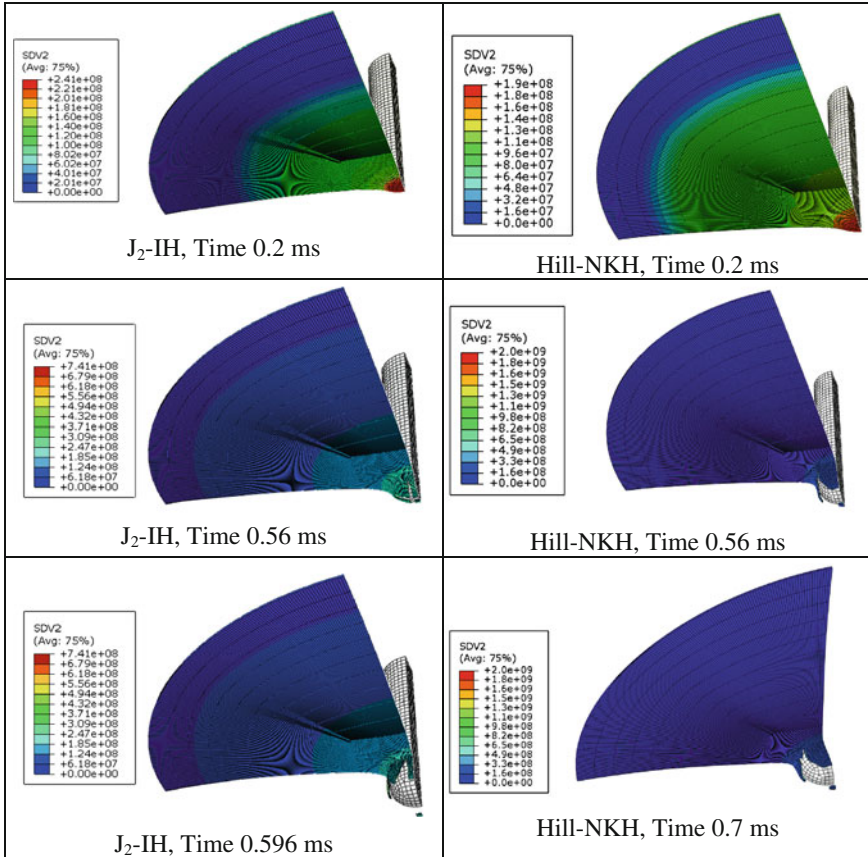


Fig. 3 Plate’s failure at different stages: pre and post perforation at velocity, $V = 25$ m/s

Fig. 4 Forces versus time curves from simulation 4 ($V_0 = 25$ m/s, $h = 0.5$ mm, $R = 70$ mm, $R_p = 6.35$ mm)

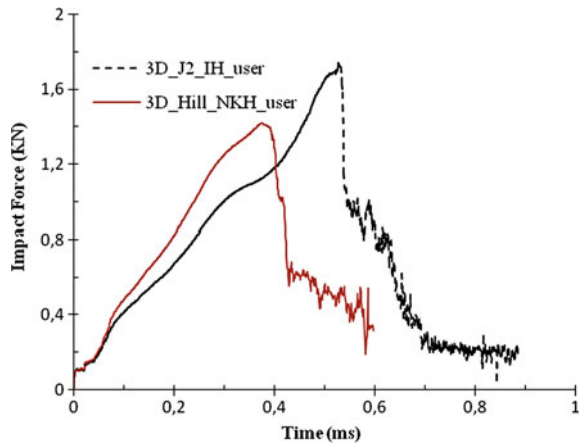
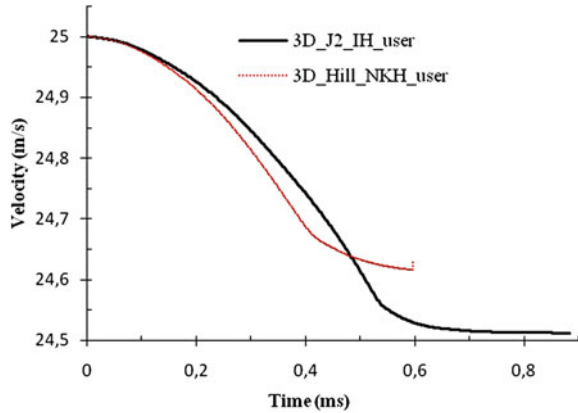


Fig. 5 Evolution of the projectile velocity during the impact



4 Conclusion

A numerical investigation has been carried out to analyze in details the perforation process of target aluminum plate when subjected to normal impact by hemispherical shape of projectile on low velocity. Numerical simulations have been performed using ABAQUS/Explicit finite element code. An elasto-viscoplastic model is implemented into a user-defined material (VUMAT) subroutine, taking into account the strain rate effect. Comparison between J_2 and Hill yield criteria with isotropic and mixed non-linear isotropic/kinematic hardening models was conducted. According to results shown, the impact region of circular target is significantly influenced by anisotropy.

References

- Abdulhamid H, Kolopp A, Bouvet C, Rivallant S (2013) Experimental and numerical study of AA5086-H111 aluminum plates subjected to impact. *Int J Impact Eng* 51:1–12
- Antoinat L, Kubler R, Barou JL, Viot P, Barrallier L (2015) Perforation of aluminium alloy thin plates. *Int J Impact Eng* 75:255–267
- Barlat F, Aretz H, Yoon JW, Karabin ME, Brem JC, Dick RE (2005) Linear transformation-based anisotropic yield functions. *Int J Plast* 21:1009–1039
- Børvik T, Clausen AH, Hopperstad OS, Langseth M (2004) Perforation of AA5083-H116 aluminium plates with conical-nose steel projectiles: experimental study. *Int J Impact Eng* 30:367–384
- Børvik T, Forrestal MJ, Hopperstad OS, Warren TL, Langseth M (2009) Perforation of AA5083-H116 aluminium plates with conical-nose steel projectiles—calculations. *Int J Impact Eng* 36:426–437
- Corran RSJ, Shadbolt PJ, Ruiz C (1983) Impact loading of plates—an experimental investigation. *Int J Impact Eng* 1:13–22

- Dean J, Dunleavy CS, Brown PM, Clyne TW (2009) Energy absorption during projectile perforation of thin steel plates and the kinetic energy of ejected fragments. *Int J Impact Eng* 36:1250–1258
- Fagerholt E, Grytten F, Gihleengen BE, Langseth M, Børvik T (2010) Continuous out-of-plane deformation measurements of AA5083-H116 plates subjected to low-velocity impact loading. *Int J Mech Sci* 52:689–705
- Grytten F, Børvik T, Hopperstad OS, Langseth M (2009) Low velocity perforation of AA5083-H116 aluminium plates. *Int J Impact Eng* 36:597–610
- Iqbal MA, Gupta NK, Sekhon GS (2006) Behaviour of thin aluminium plates subjected to impact by ogive-nosed projectiles. *Defence Sci J* 56:841–852
- Iqbal MA, Chakrabarti A, Beniwal S, Gupta NK (2010) 3D numerical simulations of sharp nosed projectile impact on ductile targets. *Int J Impact Eng* 37(1):85–195
- Jones N, Paik JK (2012) Impact perforation of aluminium alloy plates. *Int J Impact Eng* 48:46–53
- Lemaitre J, Chaboche JL (1990) *Mechanics of solid materials*. Cambridge Univ. Press
- Mars J, Wali M, Jarraya A, Dammak F, Dhiab A (2015) Finite element implementation of an orthotropic plasticity model for sheet metal in low velocity impact simulations. *Thin-Walled Struct* 89:93–100
- Mohotti D, Ngo T, Mendis P, Raman SN (2013) Polyurea coated composite aluminium plates subjected to high velocity projectile impact. *Int J Mater Des* 52:1–16
- Mohotti D, Ngo T, Raman SN, Ali M, Priyan M (2014) Plastic deformation of polyurea coated composite aluminium plates subjected to low velocity impact. *Int J Mater Des* 56:696–713
- Rodriguez-Martinez JA, Rusinek A, Pesci R, Zaera R (2012) Analysis of the strain induced martensitic transformation in austenitic steel subjected to dynamic perforation. *EDP Sci* 26. doi:[10.1051/epjconf/20122604036](https://doi.org/10.1051/epjconf/20122604036)
- Smerd R, Winkler S, Salisbury C, Worswick M, Lloyd D, Finn M (2005) High strain rate tensile testing of automotive aluminum alloy sheet. *Int J Impact Eng* 32:541–560
- Wali M, Chouchene H, Ben Said L, Dammak F (2015a) One-equation integration algorithm of a generalized quadratic yield function with Chaboche non-linear isotropic/kinematic hardening. *Int J Mech Sci* 92:223–232
- Wali M, Autay R, Mars J, Dammak F (2015b) A simple integration algorithm for a non-associated anisotropic plasticity model for sheet metal forming. *Int J Numer Meth Eng*. doi:[10.1002/nme.5158](https://doi.org/10.1002/nme.5158)
- Wilkins ML (1978) Mechanics of penetration and perforation. *Int J Eng Sci* 16:793–807